Electric Power Systems Research 202 (2022) 107572

Contents lists available at ScienceDirect

Electric Power Systems Research

journal homepage: www.elsevier.com/locate/epsr

Coordinated hierarchical voltage control for flexible DC distribution systems

Zhiyu Wei [a], Ke Peng [a,*], Chuanliang Xiao [a], Yan Li [b], Xueshen Zhao [c], Guangzeng Yao [a]

[a] School of Electrical and Electronic Engineering, Shandong University of Technology, Xincun West Road 266, Zibo, China
[b] Department of Electrical Engineering, Pennsylvania State University, University Park, PA 16802 USA
[c] Key Laboratory of Smart Grid of Ministry of Education, Tianjin University, Weijin Road 92, Tianjin, China

ARTICLE INFO

Keywords:
Flexible DC distribution systems
Dynamic performance
Steady-state performance
Coordinated hierarchical voltage control (CHVC)

ABSTRACT

The poor voltage stability and weak damping of flexible DC distribution system bring great challenges to its safe and stable operation, and its power imbalance also has a negative impact on AC distribution system. In this paper, a novel dead-zone based PID control strategy and a coordinated hierarchical voltage control (CHVC) paradigm are presented to improve the voltage stability and the damping of flexible DC distribution systems. The dead-zone based PID control is performed by a PID controller with a dead zone. It can not only carry out fast power demand response, but also prolong the service life of the battery. The CHVC strategy coordinates the battery converter control and the interconnected voltage source converter (VSC) droop control. It can not only improve the overall dynamic and steady-state characteristics of the system, but also reduce the influence of the DC system unbalanced power on the AC system. Furthermore, the effects of DC line parameters, the intensity of interconnected AC distribution systems and outer loop control parameters on the stability of the system are also analyzed, which can provide a theoretical basis for the selection of system hardware and control parameters. Numerical examples verify the feasibility and the effectiveness of CHVC.

1. Introduction

Flexible DC distribution systems enable an efficient and reliable integration of DC distributed generations and DC loads; and thus, it possesses advantages over AC distribution systems in several perspectives, such as transmission capacity, system control, and power quality [1–4]. Compared to AC distribution systems, a flexible DC distribution system is a converter-dominated network, so its stable operation is mainly realized by the control of power-electronic interfaces, such as master-slave control and droop control [5–8]. The non-differential regulation of DC voltage can be realized by master-slave control, but the master converter needs a large capacity, thus the safe and stable operation of AC distribution systems is imperatively affected by the power limit of master converter [9]. Droop control is able to coordinate the output power of each VSC, but the disadvantage is that when the load is disturbed, the DC bus voltage fluctuates greatly, leading to oscillate or even diverge [10, 11]. For this reason, battery energy storage (BES) needs to be installed to balance the power of flexible DC distribution systems.

In the recent literatures, several methods have been discussed [12–15]. in [12], the harmony search technique is proposed to optimize droop resistances, aiming at eliminating the voltage deviation caused by droop control and improving the steady-state performance of DC voltage. Further to consider the economic operation of the committed distributed generators and guaranteeing the voltage stability of the DC Microgrid under extreme condition, a distributed control strategy was proposed by [13]. For smoothing the power fluctuations between the flexible DC distribution systems and AC distribution systems, a control strategy of BES coordinated with converter stations to smooth power fluctuations is proposed in [14]. [15] discussed the DC voltage compensation control method in low-voltage system, to maintain the voltage balance by introducing the compensation of the neutral current and neutral line impedance. [16] Utilized a dynamic droop-based voltage regulation approach to address the voltage fluctuation in DC distribution systems. [17] Proposed two stabilization methods for two operation modes, and sufficient conditions for the stability of DC microgrids are obtained by identifying the eigenvalues of the Jacobian matrix. In [18], a current droop control strategy is applied to decouple the power outputs of distributed energy storage units. To combat the instability of DC distribution systems caused by constant power load,

* Corresponding author.
E-mail address: pengke@sdut.edu.cn (K. Peng).

https://doi.org/10.1016/j.epsr.2021.107572
Received 11 May 2021; Received in revised form 1 August 2021; Accepted 2 September 2021
Available online 15 September 2021
0378-7796/© 2021 Elsevier B.V. All rights reserved.

optimal allocation of BES was investigated by [19]. In [20], the influence of constant power load on the stability of DC distribution systems is analyzed by numerical continuation method, and a feed-back control method is proposed.

Although a lot of research has been done, the operation of flexible DC distribution systems is still an open problem with the most challenging ones listed as follows: (i) the transient and steady-state control of DC voltage are not unified, (ii) the voltage control capability and life expectancy of BES has not been fully considered, (iii) the primary and secondary DC voltage control are not coordinated by considering the damping enhancement. Driven by the previously mentioned motivations and advantages offered by the admittance-based methods, a novel dead-zone based PID control strategy and a coordinated hierarchical voltage control (CHVC) are proposed in this paper to resolve the aforementioned challenges, respectively. The main contributions of this paper are summarized as follows.

(1) Aim at improving the response speed of BES and prolonging service life of BES, a novel dead-zone based PID control strategy is proposed. With the dead-zone based PID control, BES can quickly respond to power demand of the flexible DC distribution system only when the DC voltage exceeds the dead zone. The frequent charging and discharging of BES are effectively suppressed by the dead-zone module; and thus, its service life can be significantly prolonged.
(2) The influence of various factors (e.g., DC line parameters, the intensity of interconnected AC distribution systems and outer loop control parameters) on the stability of the system are revealed, which provides a theoretical basis for the selection of hardware and control parameters.
(3) A coordinated hierarchical voltage control (CHVC) is presented to improve the voltage regulation capability and damping of flexible DC distribution systems. CHVC coordinates the VSC droop control and the dead-zone based PID control, which can realize primary and secondary voltage control performed by VSC and BES, respectively. The power response speed and the dynamic and steady-state characteristics of the system are improved obviously.
(4) The numerical examples of the proposed dead-zone based PID control and coordinated hierarchical voltage control coordinated hierarchical voltage control is built in DIgSILENT simulation platform, and the simulation results verify the effectiveness of the proposed control strategy.

The remainder of this paper is organized as follows. The small signal stability analysis model of flexible DC distribution systems is derived in Section 3. The instability of flexible DC distribution systems caused by the change of influencing factors is investigated. For instability caused by changes in influencing factors and improve the voltage regulation capability, the novel dead-zone based PID control and CHVC are presented in Section 4. Section 5 discusses the results of the numerical examples carried out for verification of the proposed method. Conclusions are drawn in Section 6.

2. Topology of flexible DC distribution systems

There are three main types of network configurations for flexible DC distribution systems: radial, two-terminal and multi-terminal power supply structure. The radial and two-terminal structure have the drawbacks of low power supply reliability and poor power supply capacity, so this paper mainly discusses multi-terminal flexible DC distribution systems based on VSC [21], as shown in Fig. 1.

The multi-terminal flexible DC distribution system has the following characteristics:

(1) It significantly changes the network topology of conventional AC distribution systems. Moreover, by adopting this topology, asynchronous AC systems can be flexibly interconnected, which highly improves the power supply capacity and reliability.
(2) The operation mode and network structure of flexible DC distribution systems can be flexibly controlled, and the connection and disconnection of generators and storage devices of different types and sizes are also simplified.
(3) The active power and reactive power can be decoupled independently, which enhances the power flow control ability of the system. Reactive power support can be applied to AC distribution systems, improving its fault ride-through capability.

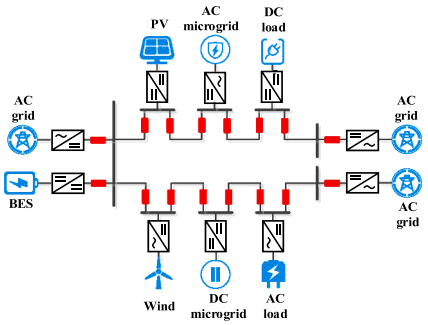

Fig. 1. Topology of multi-terminal flexible DC distribution systems.

3. Small signal stability analysis model

In the traditional control (TC) of DC distribution systems, both BES and VSC adopted droop control. The advantage of TC is that BES and VSC can suppress DC voltage fluctuation together; the disadvantage is that the damping of the system is weak and the quality of power supply is low.

3.1. Typical control characteristics

(1) U_{dc}-P_p droop control characteristic

BES usually adopts U_{dc}-P_p droop control [22], and its control expression is shown in (1):

$$P = \begin{cases} K_p\left(U_{dcref} - U_{dc}\right) + P_{ref} & if \quad P_{\min} < P < P_{\max} \\ P_{\max} & if \quad P \geq P_{\max} \\ P_{\min} & if \quad P \leq P_{\min} \end{cases} \tag{1}$$

where K_p is the DC voltage droop coefficient, P and P_{ref} are the output power of DC/DC converter and its reference value, respectively, P_{max} and P_{min} are the maximum discharging power and maximum charging power of DC/DC converter, respectively, U_{dc} and U_{dcref} are the DC voltage and its reference value, respectively.

(1) U_{dc}-I_{dc} droop control characteristic

U_{dc}-I_{dc} droop control is based on the linear relationship between DC current and DC voltage, and its control expression is shown in (2):

$$I_{dc} = \begin{cases} I_{dcref} + k\left(U_{dcref} - U_{dc}\right) & if \quad I_{dc\min} < I_{dc} < I_{dc\max} \\ I_{dc\max} & if \quad I_{dc} \geq I_{dc\max} \\ I_{dc\min} & if \quad I_{dc} \leq I_{dc\min} \end{cases} \tag{2}$$

where k is the droop coefficient; I_{dc} and I_{dcref} are the DC current and its reference value, respectively; I_{dcmin} and I_{dcmax} are the maximum output DC current of inverter and rectifier, respectively.

3.2. Small signal stability model of BES and PV power generation

BES is connected to the DC bus through DC/DC converter with U_{dc}-P_p

control, whose circuit diagram is shown in Fig. 2.

In Fig. 2, U_{dc1} and I_{dc1} are the common DC bus voltage and DC current injecting from the DC distribution systems to the DC/DC converter, respectively; U_{dc2} and I_{dc2} are the DC bus voltage at BES side and the DC current outflow from the DC/DC converter, respectively. U_g is the DC voltage of BES, R and L are the DC line resistance and inductance between BES and the DC/DC converter, respectively.

Assuming the efficiency of DC/DC converter in Fig. 2 is 100%, so the input power delivered from the dc link is equal to the output power. The controller models under U_{dc}-P_p droop control are presented in (3) to (5).

$$D = \frac{U_{dc2}}{U_{dc1}} \tag{3}$$

$$D = \left(i_{ref} - i\right)G_i(s) = \left(\left(P_{ref} - P\right)G_p(s) - i\right)G_i(s) \tag{4}$$

$$G_p(s) = K_{pp} + \frac{K_{pi}}{s}, G_i(s) = K_{ip} + \frac{K_{ii}}{s} \tag{5}$$

where, s is the Laplace operator. D is the duty cycle of the DC/DC converter, and i and i_{ref} are the current signal and its reference value, respectively.

Linearizing (4), the small signal input admittance $Y_p(s)$ of U_{dc}-P_p control can be obtained as below.

$$Y_p(s) = \frac{\left(I_{dc2(0)} + \frac{U_{dc2(0)}}{R+sL}\right)\left(\frac{U_{dc2(0)}}{U_{dc1(0)}} + K_pG_p(s)\cdot G_i(s)\right)}{\left[\left(I_{dc2(0)} + \frac{U_{dc2(0)}}{R+sL}\right)G_p(s)\cdot G_i(s) + \left(\frac{1}{R+sL}\right)G_i(s) + 1\right]} - \frac{I_{dc1(0)}}{U_{dc1(0)}} \tag{6}$$

Since the small signal stability analysis is to investigate the stability of the system at an equilibrium point, therefore, the output power of PV can be considered as a constant, and meanwhile, DC/DC converter can be modeled by using a constant power control. The small signal input admittance $Y_{pv}(s)$ of PV is equal to the model when the droop coefficient K_p is zero under U_{dc}-P_p control, as shown in (7).

$$Y_{pv}(s) = \frac{\left(I_{dc2(0)} + \frac{U_{dc2(0)}}{R+sL}\right)\frac{U_{dc2(0)}}{U_{dc1(0)}}}{\left[\left(I_{dc2(0)} + \frac{U_{dc2(0)}}{R+sL}\right)G_p(s)\cdot G_i(s) + \left(\frac{1}{R+sL}\right)G_i(s) + 1\right]} - \frac{I_{dc1(0)}}{U_{dc1(0)}} \tag{7}$$

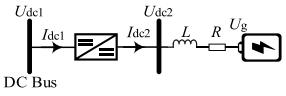

Fig. 2. Circuit diagram of BES.

3.3. Small signal stability model of VSC

The circuit diagram of VSC is shown in Fig. 3.

As shown in Fig. 3, based on the d-q frame, the current and voltage dynamic characteristics of VSC is widely available in [23].

The outer-loop and the inner-loop controller models under U_{dc}-I_{dc} droop control are presented in (8) to (11).

$$I_{dref} = \left\{I_{dcref} - k\left(U_{dcref} - U_{dc}\right) - I_{dc}\right\}G_p(s) \tag{8}$$

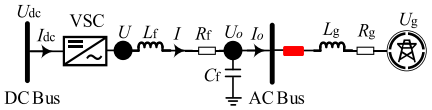

Fig. 3. Circuit diagram of VSC.

$$I_{qref} = \left(Q_{ref} - Q\right)G_p(s) \tag{9}$$

$$P_{md} = \left(I_{dref} - I_d\right)G_i(s) \tag{10}$$

$$P_{mq} = \left(I_{qref} - I_q\right)G_i(s) \tag{11}$$

where I_d and I_{dref} are the output AC current and its reference value on the d axis, respectively; I_q and I_{qref} are the AC current and its reference value on the q axis, respectively; where P_{md} and P_{mq} are the generated d-q inverter voltages to the pulse-width modulation (PWM) of VSC, respectively; Q and Q_{ref} are the reactive power and its reference value, respectively.

Applying small perturbations on current and voltage dynamic, (12) can be obtained [23].

$$U_{dc(0)}\Delta I_{dc} + I_{dc(0)}\Delta U_{dc} = \frac{3}{2}\left(\left(sC_f + \frac{1}{R_g + sL_g}\right)\left(U_{d(0)} + I_{d(0)}\left(R_f + sL_f\right)\right) + I_{d(0)}\right)\Delta U_{od} \tag{12}$$

where, Δ represent small perturbation around the operating point, and the superscript "(0)" is the steady state operating value; R_f, L_f and C_f are the resistance, inductance and capacitance of each phase line respectively; ω is the angular speed of AC voltage; R_g and L_g are the resistance and inductance of the grid, respectively.

By linearizing (8) and (10), and solving with (12), the small signal input admittance of the U_{dc}-I_{dc} droop control $Y_{con}(s)$ is obtained as shown in (13).

$$\Delta Y_{con}(s) = \frac{1.5\left(\left(sC_f + \frac{1}{R_g+sL_g}\right)\left(U_{d(0)} + I_{d(0)}\left(R_f + sL_f\right)\right) + I_{d(0)}\right)\left(\left(k + \frac{I_{dc(0)}}{U_{dc(0)}}\right)G_p(s)G_i(s) + \frac{U_{d(0)}}{U_{dc(0)}}\right)}{U_{dc(0)}\left[\left(sC_f + \frac{1}{R_g+sL_g}\right)\left(R_f + sL_f + G_i(s)\right) + 1.5G_p(s)G_i(s)\left(\left(sC_f + \frac{1}{R_g+sL_g}\right)\left(U_{d(0)} + I_{d(0)}\left(R_f + sL_f\right)\right) + I_{d(0)}\right)\right]} - \frac{I_{dc(0)}}{U_{dc(0)}} \tag{13}$$

3.4. Small signal stability model of DC load and DC line

(1) Small signal stability model of DC load

This paper discusses the DC load with constant power characteristics, the small signal input admittance $Y_{dcload}(s)$ of DC load can be shown as (14) [23].

$$\Delta Y_{dcload}(s) = \frac{\Delta I_{dcload}}{\Delta U_{dc}} = -\frac{P_{load(0)}}{U_{dc(0)}^2} \tag{14}$$

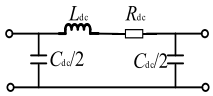

Fig. 4. Equivalent model of DC π line.

where P_{load} is the power of the constant power load. It's known from (14) that DC load shows negative admittance characteristics, which degrade the stability of the system.

(1) Small signal stability model of DC line

For DC line, π-type equivalent circuit model, shown in Fig. 4, is sufficient to meet the need of analysis. where R_{dc}, L_{dc} and C_{dc} are the DC line resistance, inductance and distributed capacitance respectively. Due to the small distributed capacitance of the DC line, the influence of the distributed capacitance of the DC line is not considered in this paper. The DC line admittance $Y_{dcline}(s)$ can be expressed as

$$\Delta Y_{dcline(s)} = \frac{1}{R_{dc} + sL_{dc}} \tag{15}$$

3.5. Advantages of input / output admittance

In multi-terminal flexible DC distribution systems, the analysis based on input / output admittance is advantageous, because the cascade input / output admittance makes it more flexible to model the add or removal of load or source without affecting the overall model equation, as shown in Fig. 5.

4. Controller design and stability analysis

A novel dead-zone based PID control and a novel coordinated hierarchical voltage control (CHVC) are proposed respectively, its advantages are as follows: (i) the transient and steady state control of DC voltage are considered together, (ii) the voltage control capability and life expectancy of battery energy storage (BES) are fully considered.

4.1. A novel dead-zone based PID control

With U_{dc}-P_p control the DC voltage signal passes through the proportional link. On the one hand, in order to improve the power regulation ability of BES, the integral link can be introduced into the outer loop controller of U_{dc}-P_p control, and the control can be defined as U_{dc}-P_{pi} control. On the other hand, in order to improve the damping capacity of BES when the DC distribution systems oscillates, the differential link can be introduced into the outer loop controller of U_{dc}-P_p control, and the control can be defined as U_{dc}-P_{pd} control. On the whole, the differential link and integral link can be introduced into the outer loop controller of U_{dc}-P_p control, and the control can be defined as U_{dc}-P_{pid} control. In addition, in view of reducing frequently charging and discharging of BES, the dead zone link is added to the above four controls, as shown in Fig. 6. where K_i and K_d are the integral gain and differential gain respectively. The stability analysis models of the four controls in Fig. 6 are obtained (details are shown in (6) and (16) ~ (18), respectively).

Based on the above small signal stability analysis model, the Nyquist diagram of the corresponding flexible DC distribution systems is obtained according to the admittance criterion. The necessary and sufficient condition for the stability of flexible DC distribution systems is that

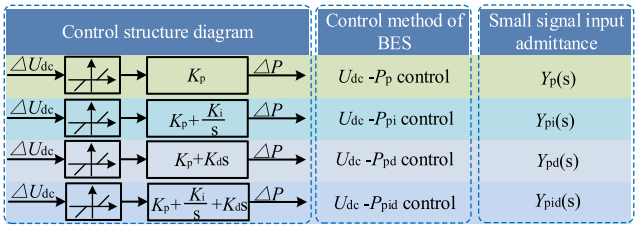

Fig. 6. Control structure diagram with different controls.

its Nyquist diagram does not encircle (–1, 0) point. If the intersection point of the Nyquist diagram and the negative real axis is on the right side of the (–1, 0) point, the stability margin of the system increases with the distance between the intersection point and the (- 1, 0) point.

$$Y_{pi}(s) = \frac{\left(I_{dc2(0)} + \frac{U_{dc2(0)}}{R+sL}\right)\left(\frac{U_{dc2(0)}}{U_{dc1(0)}} + \left(K + \frac{k_i}{s}\right)G_p(s)\cdot G_i(s)\right)}{\left[\left(I_{dc2(0)} + \frac{U_{dc2(0)}}{R+sL}\right)G_p(s)\cdot G_i(s) + \left(\frac{1}{R+sL}\right)G_i(s) + 1\right]} - \frac{I_{dc1(0)}}{U_{dc1(0)}} \tag{16}$$

$$Y_{pd}(s) = \frac{\left(I_{dc2(0)} + \frac{U_{dc2(0)}}{R+sL}\right)\left(\frac{U_{dc2(0)}}{U_{dc1(0)}} + (K + K_d s)G_p(s)\cdot G_i(s)\right)}{\left[\left(I_{dc2(0)} + \frac{U_{dc2(0)}}{R+sL}\right)G_p(s)\cdot G_i(s) + \left(\frac{1}{R+sL}\right)G_i(s) + 1\right]} - \frac{I_{dc1(0)}}{U_{dc1(0)}} \tag{17}$$

$$Y_{pid}(s) = \frac{\left(I_{dc2(0)} + \frac{U_{dc2(0)}}{R+sL}\right)\left(\frac{U_{dc2(0)}}{U_{dc1(0)}} + \left(K + \frac{K_i}{s} + K_d s\right)G_p(s)\cdot G_i(s)\right)}{\left[\left(I_{dc2(0)} + \frac{U_{dc2(0)}}{R+sL}\right)G_p(s)\cdot G_i(s) + \left(\frac{1}{R+sL}\right)G_i(s) + 1\right]} - \frac{I_{dc1(0)}}{U_{dc1(0)}} \tag{18}$$

In order to compare the system stability margin under U_{dc}-P_{pid} control and the other three controls, VSC adopts U_{dc}-I_{dc} droop control, only changing the control method of BES. The corresponding system

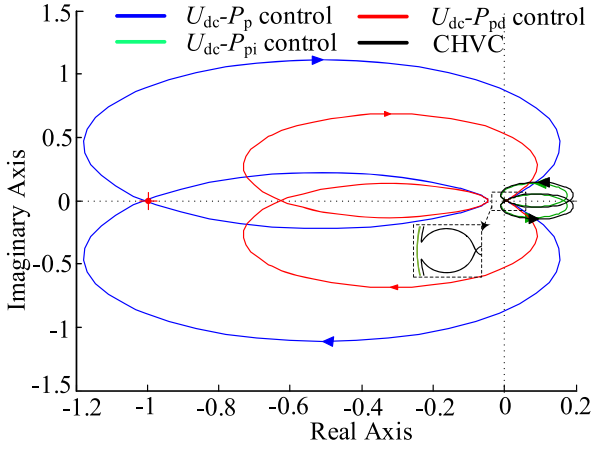

Fig. 7. Nyquist diagram with different controls.

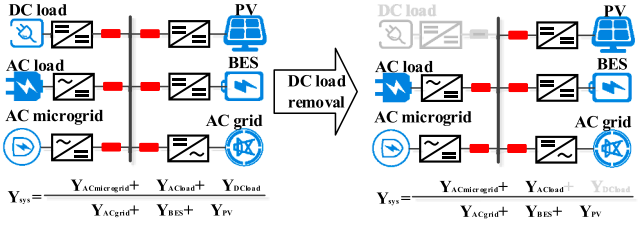

Fig. 5. Flexible DC distribution system and its equivalent admittance.

Nyquist diagrams are shown in Fig 7.

As can be seen from Fig. 7, the Nyquist diagram of the system under U_{dc}-P_p control has surrounded the (−1, 0) point, so the system has lost its stability. The intersection point of the system Nyquist diagram and the negative real axis under U_{dc}-P_{pid} control is on the right side of the (−1, 0) point, and the distance between the two points is the longest, so the stability margin of the system under U_{dc}-P_{pid} control is relatively maximum. It can be concluded that both the integral link and the differential link can effectively improve the stability margin of flexible DC distribution systems, so the U_{dc}-P_{pid} control selected in this paper. The detailed expression and control structure diagram are shown in (19) and Fig. 8, respectively.

$$P=\begin{cases}\left(K+\dfrac{K_i}{s}+K_d s\right)\left(U_{dcref}-U_{dc}\right)+P_{ref} & if \quad U_{dc}\le U_1\\ P_{ref} & if \quad U_1<U_{dc}<U_2\\ \left(K+\dfrac{K_i}{s}+K_d s\right)\left(U_{dcref}-U_{dc}\right)+P_{ref} & if \quad U_2\le U_{dc}\end{cases} \tag{19}$$

4.2. A novel coordinated hierarchical voltage control

Based on U_{dc}-P_{pid} control of BES and U_{dc}-I_{dc} droop control of VSC, CHVC is proposed in this paper. The control structure diagram for TC and CHVC is shown in Fig. 9.

As can be seen from Fig. 9, the primary voltage control shall be undertaken by VSC in order to achieve the following purposes: (i) VSCs shall coordinate the output power with each other and give full play to its voltage regulating capacity; (ii) reduce the burden of voltage regulation of BES, restraining the phenomenon of frequent charging and discharging in BES.

Although the primary voltage regulation can respond at any given time, when the power imbalance of flexible DC distribution systems is serious, the output power of VSC is not enough to meet the power requirement of the system. At this time, BES is required to perform secondary voltage control to compensate the unbalanced power of the system.

The secondary voltage control is completed by BES under U_{dc}-P_{pid} control to achieve the following objectives: (i) to better meet the power demand of flexible DC distribution systems, so that the DC voltage can be restored to the stable working area after the secondary voltage control; (ii) enhance system damping, speeding up the system dynamic adjustment and improving system stability; (iii) suppresses the unplanned instantaneous fluctuation of VSC output power, and the friendly grid connection of the flexible DC distribution systems is realized.

This paper uses dead zone-based U_{dc}-P_{pid} control, which is mainly based on the following considerations. The power imbalance of flexible DC distribution systems is all borne by BES, and the VSC compensates for the power imbalance only when BES reaches the upper limit, and has the following drawbacks: (i) BES is frequently charging and discharging, and its life expectancy will be greatly affected; (ii) The voltage control capability of VSC is not fully utilized, and the burden on BES is too heavy.

4.3. Stability analysis under the change of parameters

Based on the above small signal stability analysis model of flexible DC distribution systems, the comparison of stability margin between TC and CHVC is investigated in this paper, considering the changes of DC line parameters, intensity of interconnected AC distribution systems and outer loop control parameters. The corresponding system Nyquist

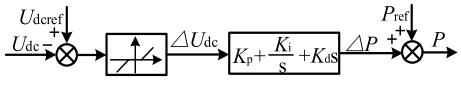

Fig. 8. The control structure diagram of U_{dc}-P_{pid} control.

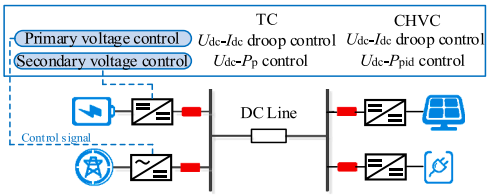

Fig. 9. The control structure diagram for TC and CHVC.

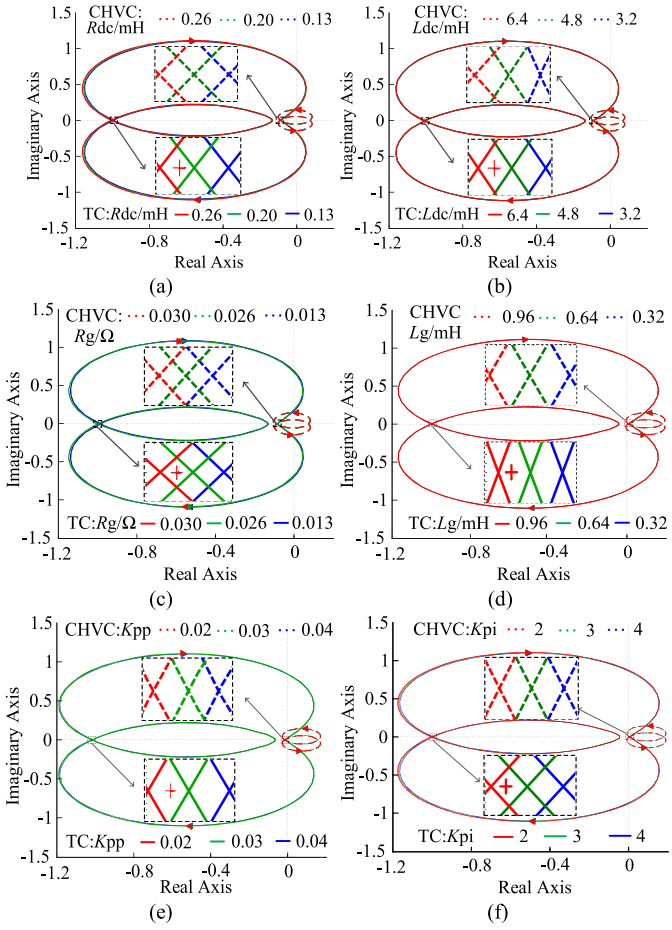

Fig. 10. The Nyquist diagram of the system under the change of the following factors: (a) DC line resistance, (b) DC line inductance, (c) AC line resistance, (d) AC line inductance, (e) the proportional gain, (f) the integral gain.

diagrams are shown in Fig 10.

Taking the resistance parameters of DC line as an example, the process of stability analysis is introduced in detail. Assuming that the DC line inductance is constant, when the DC line resistance varies from 0.13 Ω to 0.26 Ω, that is, when the DC line length varies from 1 km to 2 km, the system's stability margins of CHVC and TC is compared as shown in Fig 10(a).

As can be seen from Fig. 10(a): (i) with the increase of DC line resistances, the intersection of the system Nyquist diagram and the negative real axis gradually moves to the left, inducing the decease of the stability margin; (ii) under CHVC, high stability margins can be obtained compared to TC as DC line resistance varies from 0.13 Ω to 0.26 Ω; (iii) when DC line resistance is 0.26 Ω, the system is stable under CHVC, but it is unstable under TC.

To sum up, "(i) In certain intervals, the stability margin of the system will decrease with the increase of the DC line parameters, the weakening of AC distribution systems and the decrease of the outer loop control

parameters. Overall, the system parameter mismatch problem will cause the system stability to decrease. (ii) the stability margin of flexible DC distribution systems under TC is small, and even unstable in serious cases, while the flexible DC distribution systems under CHVC has larger stability margin.

5. Evaluation results

Based on the IEEE33-node text system, a three-terminal flexible DC distribution system is added, as shown in Fig. 11.

The flexible DC distribution systems integrates PV power generation, BES and AC / DC load. DC voltage level is 20 kV. The rated capacity of PV generator is 2MW. The rate capacity of BES is 2MW. DC load power is 2MW. With DIgSILENT software the modified IEEE 33-node test system is built. The control parameters are given in Tables 1 and 2. It should be noted that the control parameters of U_{dc}-P_{pi} control and U_{dc}-P_{pd} control can be reflected in U_{dc}-P_{pid} control, so only the control parameters of U_{dc}-P_{pid} control are given.

5.1. Validation of CHVC

At 1 s, due to the sudden reduction of sunlight, the power of PV is immediately reduced to 50% of the current output, and the simulation ends at 19 s. The simulation results of the four controls are shown in Fig. 12.

When the output power of PV power generation drops suddenly, there is a large power shortage in DC distribution systems.

Based on U_{dc}-P_p control, the power regulation of BES is relatively small, that is, the control can't give full play to its power regulation ability. The dynamic regulation process of the system is relatively long. After the transient regulation, the steady-state DC voltage deviates far from the set point. The operation point of each VSC changes greatly, inducing the instantaneous power exchange between AC and DC systems and great fluctuations of the AC system voltage.

Under CHVC and U_{dc}-P_{pi} control, BES can quickly change its power output, giving full play to its power regulation ability against this kind of small disturbance. The dynamic regulation process of the system is relatively short. At the end of the transient regulation process, the steady-state DC voltage is close to the set point and system power quality is improved. The operation point of each VSC has a small change, that is, the instantaneous change of switching power between AC and DC systems is small, and the voltage level of AC system is less affected.

Under CHVC, the dynamic regulation process is accelerated, that is, the dynamic performance of the system is enhanced. However, after the end of the transient process, the steady state of the system is consistent with U_{dc}-P_p control.

From the above theoretical analysis, it can be seen that the damping of the DC distribution system under CHVC is stronger than that of U_{dc}-P_{pi} control. For further verification, under another group of control parameters and a large oscillation of load shedding, the simulation results of the two controls are shown in Fig. 13.

Under CHVC control, BES can quickly change its power output,

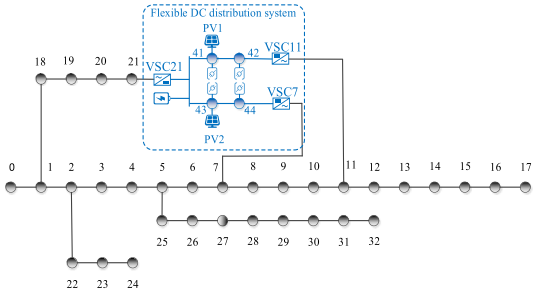

Fig. 11. The modified IEEE 33-node test system.

Table 1
Control parameters of U_{dc}-I_{dc} droop control.

The inner-loop controller	K_{ipd} 0.04	K_{iid} 4	The outer-loop controller	K_{ppP} 0.6	K_{piP} 60	The droop control controller	k 5
	K_{ipq} 0.04	K_{iiq} 4		K_{ppQ} 0.6	K_{piQ} 60		

Table 2
Control parameters of U_{dc}-P_{pid} control.

The inner-loop controller		The outer-loop controller		The PID controller		
K_{ip}	K_{ii}	K_{pp}	K_{pi}	K_p	K_i	K_d
0.04	4	0.6	60	2	30	5

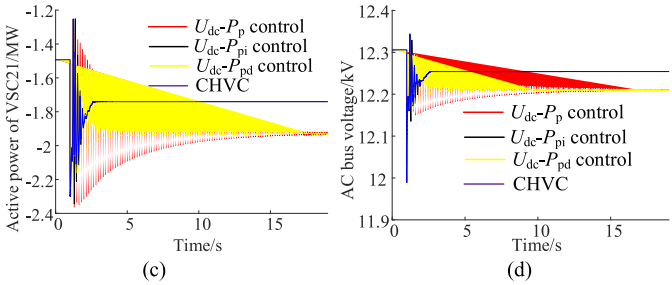

Fig. 12. The simulation results of the three controls: (a) the output power of BES, (b) DC voltage, (c) the active power of VSC21, (d)the AC voltage of VSC21.

giving full play to its power regulation ability. The system has a larger stability margin to ensure the stability of the DC bus voltage. At the end of the transient regulation process, the steady-state DC voltage is close to the set point. The operation point of each VSC has a small change, that is, the instantaneous change of switching power between AC and DC systems is small, and the voltage level of AC system is less affected.

However, under U_{dc}-P_{pi} control, the system does not have enough stability margin, the DC voltage oscillates continuously and can't converge to the steady state.

Furthermore, the dead-zone based PID control can avoid frequently battery power adjustment against small disturbance, and provide damping to keep stable when large oscillation occurs, as shown in Fig. 14.

Based on U_{dc}-P_{pid} control of BES and U_{dc}-I_{dc} droop control of VSC, CHVC is proposed in this paper. It is necessary to verify the correctness of the above theoretical analysis, so the simulation results of changing DC line parameters, the intensity of interconnected AC distribution systems and outer loop control parameters will be given, and the control effects of TC and CHVC will be compared and analyzed.

5.2. Simulation verification under the change of parameters

The simulation results of the negative effects of DC line parameters, the intensity of interconnected AC distribution systems and outer loop control parameters on the stability of the system are shown in Fig. 15.

Taking the resistance parameters of DC line as an example, the simulation process is introduced in detail. Assuming that the DC line inductance is constant, when the DC line resistance varies from 0.26 Ω to 0.52 Ω, that is, when the DC line length varies from 2 km to 4 km, the simulation waveform is shown in Fig. 15(a).

From Fig. 15(a), it can be seen that under the same PV power disturbance, when the DC line resistance is equal to 0.26 Ω, the system produces a stable response under TC. But the DC voltage is at a lower level after the secondary voltage control, and the dynamic regulation process of the system is relatively long. However, when the DC line resistance is equal to 0.52 Ω, the DC voltage oscillates and diverges

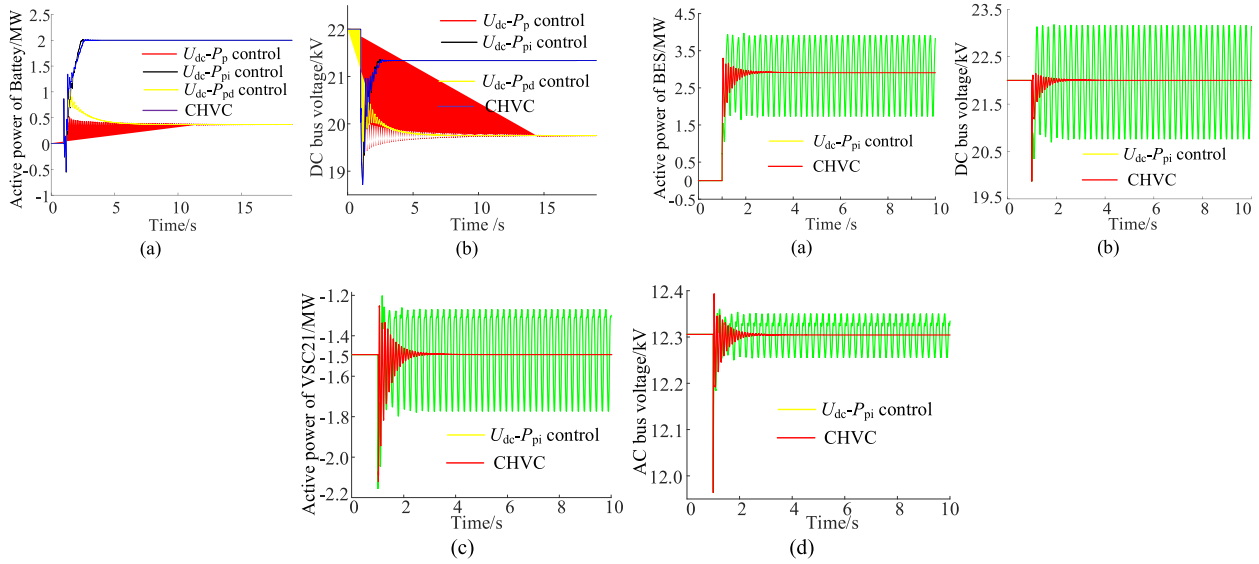

Fig. 13. The simulation results of the two controls: (a) the output power of BES, (b) DC voltage, (c) the active power of VSC21, (d)the AC voltage of VSC21.

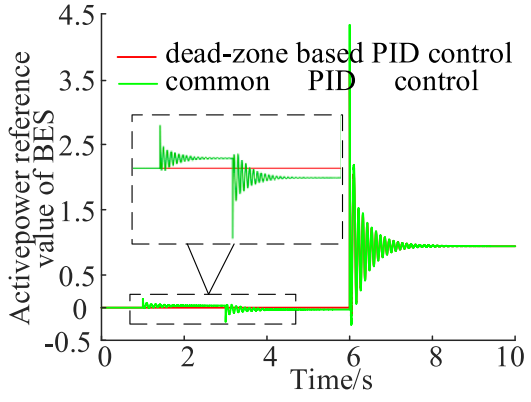

Fig. 14. The simulation curves of the output power reference value of BES.

under TC, and the system loses its stability. In contrast, under CHVC, system stability margin is improved and the DC voltage quickly recovers to the allowable range after the secondary voltage control, the dynamic regulation process of the system is relatively short.

To sum up, (i) the damping and stability margin of the system will decrease with the increase of the DC line parameters, the weakening of AC distribution systems and the decrease of the outer loop control parameters. (ii) When the power imbalance of DC distribution systems is serious, TC can't meet the power requirements of the system, and can't provide enough damping to maintain DC voltage stability, inducing the system loses stability. (iii) CHVC proposed in this paper can increase system stability margin and effectively restrain the occurrence of power imbalance and DC voltage fluctuation in DC distribution systems. Moreover, it can reduce the influence on AC distribution systems.

6. Conclusion

This paper proposes a novel coordinated hierarchical voltage control (CHVC), with the aim of improving the transient and steady state performance of flexible DC distribution systems. The primary voltage control is performed by voltage source converter (VSC) based on U_{dc}-I_{dc} droop control, and the secondary voltage control is performed by BES based on a novel dead-zone based PID control. The conclusions are as follows:

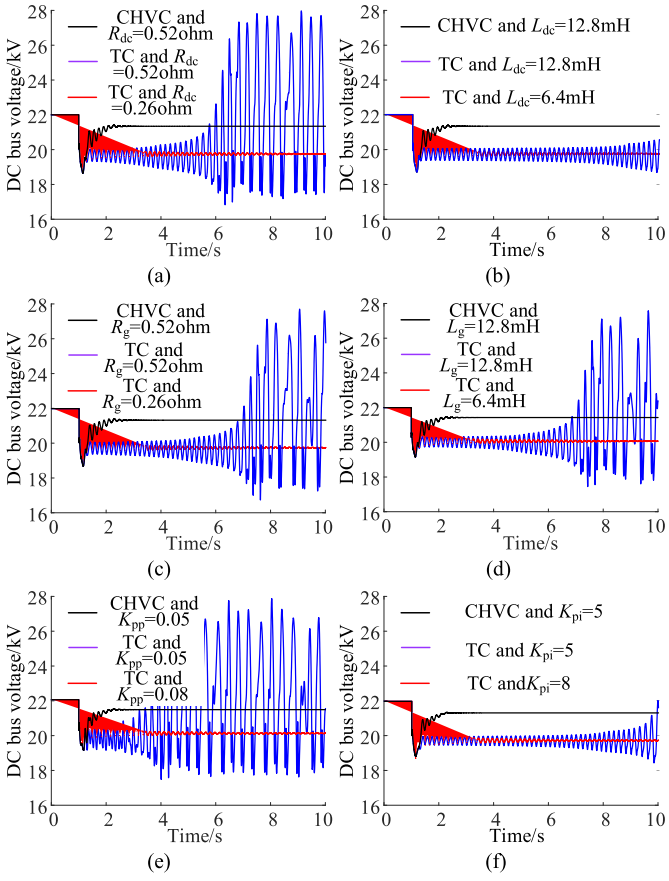

Fig. 15. The simulation results of DC voltage under the change of the following factors: (a) DC line resistance, (b) DC line inductance, (c) AC line resistance, (d) AC line inductance, (e) the proportional gain, (f) the integral gain.

(1) The increase of DC line parameters, the weakening of AC distribution systems and the decrease of the outer loop control parameters would lead to the decrease of the system damping and stability.

(2) Under CHVC designed in this paper, BES can quickly respond to the power demand of flexible DC distribution systems when the DC voltage exceeds the dead zone. Theoretical and simulation results show that CHVC has the following advantages: (i) the damping and stability of the system have been significantly improved, (ii) the transient regulation process is significantly shortened, which is due to the rapid power response of BES when the DC voltage exceeds the dead zone, (iii) the steady DC voltage can be restored to the allowable range after secondary voltage regulation, (iv) the negative impact on the stable operation of AC distribution systems, caused by the power imbalance of DC distribution, is also significantly suppressed.

CRediT authorship contribution statement

Zhiyu Wei: Data curation, Investigation, Resources, Software, Validation, Writing – original draft. **Ke Peng:** Conceptualization, Methodology, Project administration, Funding acquisition. **Chuanliang Xiao:** Writing – review & editing, Supervision. **Yan Li:** Writing – review & editing, Supervision. **Xueshen Zhao:** Software, Validation, Supervision. **Guangzeng Yao:** Visualization, Supervision.

Declaration of Competing Interest

The authors declared that they have no conflicts of interest to this work.

Acknowledgments

This work is supported by National Nature Science Foundation of China (51807112)

References

[1] D.M. Zhao, H.X. Wang, R. Tao, Multi-time scale dispatch approach for an AC/DC hybrid distribution system considering the response uncertainty of flexible loads, Electr. Power Syst. Res. 199 (1) (2021), 107394.
[2] J. King, J. Berry, N. Murdoch, Steady-state modelling for the integration of a bi-directional AC–DC–AC flexible power link, CIRED - Open Access Proc. J. 1 (2017) 445–449.
[3] M. Li, K. Jia, T. Bi, et al., Sixth harmonic-based fault location for VSC-DC distribution systems, IET Gener. Transm. Distrib. 11 (14) (2017) 3485–3490.
[4] Y.C. Yang, C. Huang, DC fault location in multi-terminal DC distribution network based on voltage similar triangle principle, Electr. Power Syst. Res. 184 (2020), 106306.
[5] G.Z. Yao, K. Peng, X.D. Li, S.H. Jiang, Y.Q. Liu, A reduced-order model for high-frequency oscillation mechanism analysis of droop control based flexible DC distribution system, Int. J. Electr. Power Energy Syst. 130 (2021), 106927.
[6] X.S. Zhao, K. Peng, Q. Wan, et al., Research on droop control strategy of multi-terminal AC/DC hybrid distribution system, Energy Procedia 145 (2018) 54–63.
[7] Y.C. Liu, X.Z. Zhuang, Q.J. Zhang, et al., A novel droop control method based on virtual frequency in DC microgrid, Int. J. Electr. Power Energy Syst. 119 (2020), 105946.
[8] Y. Xu, J. Liu, Analysis of pole-to-pole fault characteristics of flexible DC system and design of current-limiting device, J. Eng. 13 (2017) 1546–1549.
[9] Y. Wang, Q. Song, B. Zhao, et al., Analysis and optimisation of modulation strategy based on dual-phase-shift for modular multilevel high-frequency-link DC transformer in medium-voltage DC distribution network, IET Power Electron. 11 (2) (2018) 253–261.
[10] X. Li, M. Zhu, G. He, et al., DC power collection system for PV station based on impedance-source multi-module DC–DC step-up converter, J. Eng. (13) (2017) 1734–1739.
[11] F. Chen, R. Burgos, D. Boroyevich, et al., Investigation of nonlinear droop control in DC power distribution systems: load sharing, voltage regulation, efficiency, and stability, IEEE Trans. Power Electron. 34 (10) (2019) 9404–9942.
[12] M. Mokhtar, M.I. Marei, A.A. El-Sattar, Improved current sharing techniques for DC microgrids," electric power components and systems, Electr. Power Compon. Syst. 46 (7) (2018) 757–767.
[13] W. Hatahet, M. Mokhtar, M.I. Marei, Performance recovery control of grid-connected DC microgrid, Int. J. Electr. Power Energy Syst. 130 (2021) 3032–3045.
[14] H. Zhang, Z. Yuan, Y. Zhao, et al. 2015. "A strategy of battery energy storage system coordinated with converter stations for smoothing power fluctuations of flexible DC distribution system." Paper Presented At International Conference On Renewable Power Generation (RPG 2015), Beijing. October 17-18.
[15] T. Jung, G. Gwon, C. Kim, et al., Voltage regulation method for voltage drop compensation and unbalance reduction in bipolar low-voltage DC distribution system, IEEE Trans. Power Delivery 33 (1) (2018) 141–149.
[16] R. Krishan, A. Verma and S. Mishra. 2017. "Voltage regulation of residential DC distribution feeder using coordinated battery energy storage units." Paper Presented At the 2017 IEEE International Conference On Smart Grid and Smart Cities (ICSGSC), Singapore. July 23-26.
[17] M. Su, Z. Liu, Y. Sun, et al., Stability analysis and stabilization methods of DC microgrid with multiple parallel-connected DC–DC converters loaded by CPLs, IEEE Trans. Smart Grid 9 (1) (2018) 132–142.
[18] C. Shi, X. Tang, G. Zhang, et al. 2017. "Research on power sharing control strategy in distributed energy storage system-based DC distribution network." Paper Presented At the 2017 Chinese Automation Congress (CAC), Jinan. October 20-22.
[19] G. Song, X. Huang, T. Wang, et al., Scheme to improve the load characteristics in DC distribution networks based on optimal allocation of energy storage systems, J. Eng. 13 (2017) 2461–2465.
[20] S. Grillo, V. Musolino, G. Sulligoi, et al. 2012. "Stability enhancement in DC distribution systems with constant power controlled converters." Paper Presented At 2012 IEEE 15th International Conference On Harmonics and Quality of Power, Hong Kong. June 17-20.
[21] G. Jing, A. Zhang, H. Zhang, et al. 2019. "A strategy of battery energy storage system coordinated with converter stations for smoothing power fluctuations of flexible DC distribution system." Paper Presented At 2019 Chinese Control And Decision Conference, Nanchang. June 3-5.
[22] S.M. Malik, Y.Y. Sun, W. Huang, et al., A Generalized droop strategy for interlinking converter in a standalone hybrid microgrid, Appl. Energy 226 (2018) 1056–1063.
[23] K. Peng, Z.Y. Wei, J.J. Chen, et al., Hierarchical virtual inertia control of DC distribution system for plug-and-play electric vehicle integration, IEEE Trans. Smart Grid 128 (2021), 106769.

Zhiyu Wei received his B.*Sc.* degree in electrical engineering from Shandong University of Technology, China, in 2018. He is currently working toward the M.*Sc.* degree in electrical engineering at Shandong University of Technology, China. His-research interests include stability analysis and optimal control of flexible DC distribution system.

Ke Peng received the B.S. degree from China University of Mining and Technology, Xuzhou, China, in 2006, and the Ph.D. degree in electrical engineering from Tianjin University, Tianjin, China, in 2012. He is an Associate Professor at Shandong University of Technology. His-research field includes distributed generation system simulation, AC-DC smart distribution system.

Chuanliang Xiao received the B.Eng. degree in the School of Electrical Engineering and Automation from Hefei University of Technology, Hefei, China, in 2015, and the Ph.D. degree in the School of Electrical Engineering and Automation from Hefei University of Technology, Hefei, China, in 2020. He is currently a Lecturer in the School of Electrical and Electronic Engineering, Shandong University of Technology, Zibo, China. His-research interests include renewable energy, distributed generation.

Yan Li received the B.*Sc*. and M.*Sc*. degrees in electrical engineering from Tianjin University, Tianjin, China, in 2008 and 2010, respectively. She is currently working toward the Ph.D. degree in electrical engineering at the University of Connecticut, Storrs, CT, USA. Her research interests include microgrids and networked microgrids, formal analysis, power system stability and control, software-defined networking, and cyber-physical security.

Xueshen Zhao received the B.*Sc*. and M.*Sc*. degrees in electrical engineering from Shandong University of Technology, Shandong, China, in 2016 and 2019, respectively. He is currently working toward the Ph.D. degree in the School of Electrical and Information Engineering, Tianjin University, Tianjin, China. His-research interests include stability analysis and optimal control of flexible DC distribution system.

Guangzeng Yao received his B.*Sc*. degree in electrical engineering from Qufu Normal University, Rizhao, China, in 2019. He is currently working towards M.*Sc*. degree in electrical engineering at Shandong University of Technology, Zibo, China. His-research interests include stability analysis and optimal control of flexible DC distribution system.